ELSEVIER

Journal of Alloys and Compounds 370 (2004) 114–122

Journal of ALLOYS AND COMPOUNDS

www.elsevier.com/locate/jallcom

A computational thermodynamic model of the Ca–Mg–Zn system

Carl O. Brubaker*, Zi-Kui Liu

Department of Materials Science and Engineering, The Pennsylvania State University, 107 Steidle Building, University Park, PA 16802, USA

Received 17 July 2003; accepted 20 August 2003

Abstract

The phase equilibria and thermodynamic properties of the Mg–Ca–Zn ternary system were analyzed and a complete thermodynamic description of the system was obtained using a computerized optimization procedure. Based on the experimental data, one ternary intermetallic compound was considered for the model, while another ternary intermetallic compound was speculated. The calculated results were compared with the experimental data in the literature.

Keywords: Thermodynamic modeling; Phase diagrams; Metals and alloys

1. Introduction

Calcium and zinc are two alloying elements used in magnesium-based alloys. A thermodynamic description of the Mg–Ca–Zn ternary system is needed for the development of a thermodynamic database for the further refinement of existing magnesium-based alloys and the development of new ones. The present work contributes to the thermodynamic database of magnesium alloy systems.

To create an accurate thermodynamic model of a ternary system, it is necessary to first have thermodynamic descriptions of the three constituent binary systems. Computational thermodynamic modeling of the Mg–Ca, Mg–Zn, and Ca–Zn systems has been reported in the literature [1–3]. The calculated phase diagrams for the three binary systems are shown in Figs. 1–3, respectively. The Mg–Ca system has one intermediate phase, and neither magnesium nor calcium display any solubility in one another. The Mg–Zn system has five intermediate phases. There is no solubility of magnesium in zinc, but there is a small amount of solubility of zinc in magnesium. The Ca–Zn system contains eight intermetallic phases. Neither calcium nor zinc displays any solubility in one another. Most of the intermediate phases were modeled as stoichiometric compounds, except the Laves phases Mg_2Ca and $MgZn_2$ in the Mg–Ca and Mg–Zn systems. Thermodynamic data for the pure elements were taken from the compilation of Dinsdale [4]. Crystallographic data for the phases of the three binary systems are listed in Appendix A.

2. Experimental data

The Mg–Ca–Zn phase diagram is based largely on the work of Paris [5], who investigated the system by measuring the cooling curves of 189 different alloys. Paris selected his alloy compositions such that the cooling curve data could be plotted as sixteen isopleths (see Fig. 4). Based on the cooling curves and metallography, Paris claimed to have found one ternary compound that he named $Ca_2Mg_5Zn_5$ [5,6], but did not report the crystallographic data for the compound.

The isothermal section of the Mg–Ca–Zn system at 335 °C was investigated by Clark, using metallography and X-ray diffraction [7]. Clark found evidence of two ternary compounds, namely β ($Ca_2Mg_6Zn_3$) and ω ($Ca_2Mg_5Zn_{13}$), and refuted Paris' nomenclature of $Ca_2Mg_5Zn_5$, whose location roughly corresponds to Clark's β compound [7–9]. Although there are Joint Committee on Powder Difraction Standards (JCPDS) cards filed by Clark for the phases $Ca_2Mg_6Zn_3$ and $Ca_2Mg_5Zn_{13}$ [8,9], there is nothing in the literature published by Clark to support those particular compositions. The *Handbook of Ternary Alloy Phase Diagrams* listed Clark's β and ω compounds as "?$CaMg_2Zn$" and "?$Ca_2Mg_5Zn_{13}$", respectively [10].

* Corresponding author. Present address: Code 50, 2008 Stump Neck Road, Indian Head, MD 20602, USA. Tel.: +1-301-7446850x258.
E-mail address: carlbrubaker@excite.com (C.O. Brubaker).

0925-8388/$ – see front matter © 2003 Elsevier B.V. All rights reserved.
doi:10.1016/j.jallcom.2003.08.097

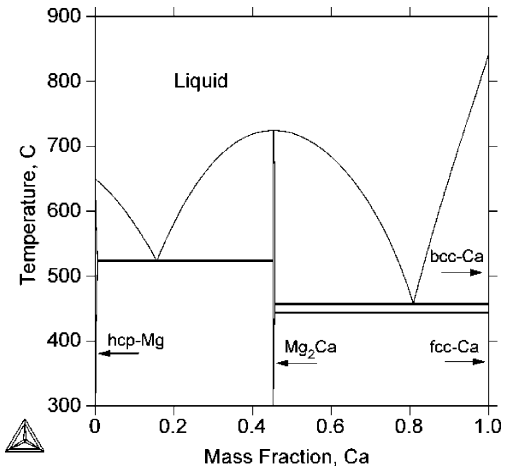

Fig. 1. The calculated Ca–Mg phase diagram [1].

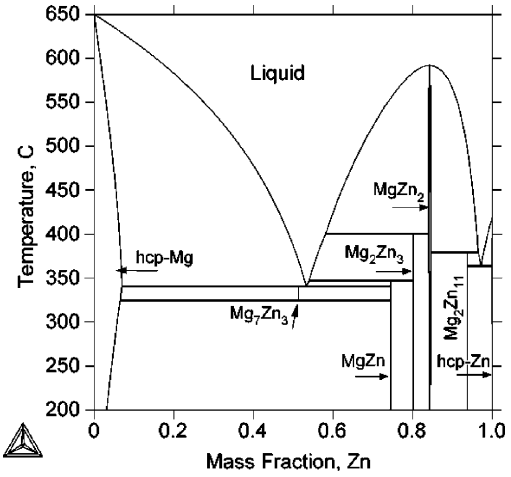

Fig. 2. The calculated Mg–Zn phase diagram [2].

Jardim et al. studied a melt-spun Mg–Ca–Zn alloy using transmission electron microscopy, energy dispersive X-ray spectroscopy and scanning transmission electron microscopy [11]. They found precipitates in the heat-treated alloy, and determined that the composition of the precipitates is $Ca_2Mg_6Zn_3$, which is the same as the composition given on the JCPDS card filed by Clark [8]. They also reported the crystal structure of the ternary compound (see Appendix A), and did not find evidence of a second ternary compound.

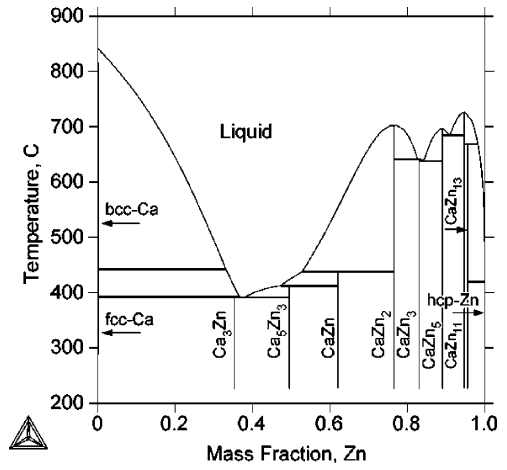

Fig. 3. The calculated Ca–Zn phase diagram [3].

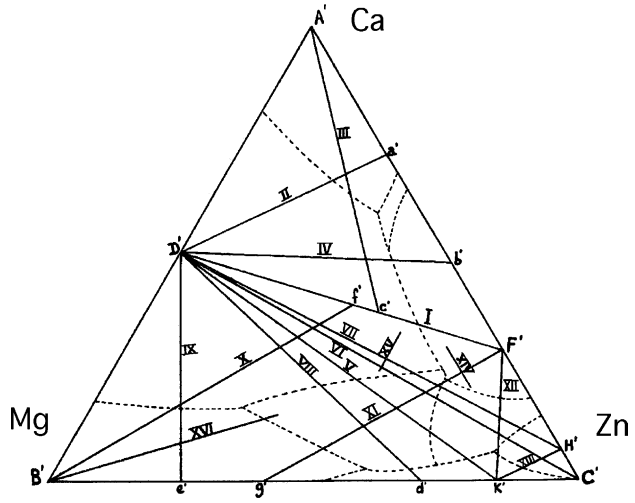

Fig. 4. The liquidus projection of the Mg–Ca–Zn ternary system, as drawn by Paris, with the locations of his sixteen isopleths superimposed [6]. The axes are in mass fraction.

The ternary compound $Ca_2Mg_6Zn_3$ was included in the computational modeling of the system. The ω compound reported by Clark, with a composition of $Ca_2Mg_5Zn_{13}$, was speculated due to the limited experimental data available.

3. Thermodynamic models

One intermetallic compound was considered for the Mg–Ca–Zn system. Although Clark's work indicates a homogeneity range for the phase, it was modeled as a stoichiometric compound due to the lack of a specific composition range. The system was optimized using both the composition of Paris, i.e. $Ca_2Mg_5Zn_5$, and that given by Clark and Jardim et al., $Ca_2Mg_6Zn_3$. The ternary compound's Gibbs energy function is written as

$$^{\circ}G_m^{Ca_xMg_yZn_z} = x^{\circ}G_{Ca}^{fcc} + y^{\circ}G_{Mg}^{hcp} + z^{\circ}G_{Zn}^{hcp} + a + bT \quad (1)$$

where $^{\circ}G_{Ca}^{fcc}$, $^{\circ}G_{Mg}^{hcp}$, and $^{\circ}G_{Zn}^{hcp}$ are the Gibbs energies of the pure elements [4]. The parameters *a* and *b* are to be evaluated from experimental data. The reference state of the Gibbs energy of individual phases is the so-called standard element reference (SER), i.e. the enthalpies of the pure elements in their stable states at 298.15 K.

The solution phases, liquid, fcc, bcc, and hcp, were treated as a substitutional solution, with the Gibbs energy expressed as

$$G_m^{\Phi} = \sum x_i {}^{\circ}G_i^{\Phi} + RT\sum x_i \ln x_i + {}^{xs}G_m^{\Phi} \quad (2)$$

where Φ represents liquid, bcc, fcc, or hcp, and i is Ca, Mg, or Zn. The term ${}^{xs}G_m^{\Phi}$ is the excess Gibbs energy, expressed in Redlich–Kister polynomials [12],

$$ {}^{xs}G_m^{\Phi} = \sum_i \sum_{j>i} x_i x_j \sum_{k=0}^{n} {}^{k}L_{i,j}^{\Phi}(x_i - x_j)^k + x_{Ca}x_{Mg}x_{Zn}L_{Ca,Mg,Zn}^{\Phi} \quad (3) $$

where ${}^{k}L_{Ca,Zn}^{\Phi}$, ${}^{k}L_{Mg,Zn}^{\Phi}$, and ${}^{k}L_{Ca,Mg}^{\Phi}$ are the binary interaction parameters taken from the constituent binary systems, and $L_{Ca,Mg,Zn}^{\Phi}$ is a ternary interaction parameter with the following form:

$$ L_{Ca,Mg,Zn}^{\Phi} = x_{Ca}{}^{0}L_{Ca,Mg,Zn}^{\Phi} + x_{Mg}{}^{1}L_{Ca,Mg,Zn}^{\Phi} + x_{Zn}{}^{2}L_{Ca,Mg,Zn}^{\Phi} \quad (4) $$

where ${}^{j}L_{Ca,Mg,Zn}^{\Phi} = {}^{j}a + {}^{j}bT$, and ${}^{j}a$ and ${}^{j}b$ are model parameters to be evaluated from experimental information. The expression $j > i$ in the term $\sum_{j>i}$ indicates that component j must come after component i alphabetically.

Two phases in the Mg–Ca and Mg–Zn systems, namely Mg_2Ca and $MgZn_2$, have the same Laves crystal structure, and can be said to be one phase with a highly variable composition in the Mg–Ca–Zn ternary system (see Appendix A). The Laves phase was modeled with two sublattices, with 0.66667 sites in the first sublattice, and 0.33333 sites in the second sublattice. To fully describe the Laves phase, it must be modeled such that all three elements occupy both sublattices, i.e. $(Mg,Ca,Zn)_{0.66667}(Mg,Ca,Zn)_{0.33333}$. The Gibbs energy of the Laves phase is thus expressed as

$$ \begin{aligned} G_m = {} & \sum_i \sum_j y_i^{I} y_j^{II} {}^{\circ}G_{i:j} + 0.66667RT\sum_i y_i^{I} \ln y_i^{I} \\ & + 0.33333RT\sum_i y_i^{II} \ln y_i^{II} + \sum_i \sum_{j>i} \sum_k y_i^{I} y_j^{I} y_k^{II} L_{i,j:k} \\ & + \sum_i \sum_{j>i} \sum_k y_k^{I} y_i^{II} y_j^{II} L_{k:i,j} \\ & + \sum_i y_{Ca}^{I} y_{Mg}^{I} y_{Zn}^{I} y_i^{II} L_{Ca,Mg,Zn:i} \\ & + \sum_i y_i^{I} y_{Ca}^{II} y_{Mg}^{II} y_{Zn}^{II} L_{i:Ca,Mg,Zn} \end{aligned} \quad (5) $$

where y_i^{I} and y_i^{II} are the site fractions of i in the first and second sublattices, respectively, and ${}^{\circ}G_{i:j}$ is the Gibbs energy of the end member compound $i_{0.66667}\ j_{0.33333}$. The letters i, j and k may represent Ca, Mg, or Zn. The term $L_{i:j,k}$ is an interaction parameter, with a colon separating elements in different sublattices, and a comma separating elements interacting with each other in the same sublattice.

Using first-principle calculations, the lattice stabilities of pure calcium, magnesium, and zinc in the Laves structure have been determined to be [13]

$$ {}^{\circ}G_{Ca:Ca} = 12330 + {}^{\circ}G_{Ca} \quad (6) $$

and

$$ {}^{\circ}G_{Mg:Mg} = 7720 + {}^{\circ}G_{Mg} \quad (7) $$

and

$$ {}^{\circ}G_{Zn:Zn} = 5000 + {}^{\circ}G_{Zn} \quad (8) $$

The Gibbs energy for the Mg_2Ca phase, namely ${}^{\circ}G_{Mg:Ca}$, is taken from the Mg–Ca database [1]. Based on first-principles calculations [13], the expression for ${}^{\circ}G_{Ca:Mg}$ was set to be

$$ {}^{\circ}G_{Ca:Mg} = 26650 + 0.66667{}^{\circ}G_{Ca} + 0.33333{}^{\circ}G_{Mg} \quad (9) $$

Although $CaZn_2$ is a stable phase in the Mg–Ca–Zn system, it is not a Laves phase. Nevertheless, to fully describe the Laves phase in the Mg–Ca–Zn system, there must be a set of Gibbs energies to represent the hypothetical Laves phase consisting only of calcium and zinc. Without knowing anything about Ca_2Zn and $CaZn_2$ as they would exist in the Laves crystal structure, and from the first-principles calculations of ${}^{\circ}G_{Ca:Mg}$ [13], it was assumed that

$$ {}^{\circ}G_{Ca:Zn} = 26650 + 0.66667{}^{\circ}G_{Ca} + 0.33333{}^{\circ}G_{Zn} \quad (10) $$

and

$$ {}^{\circ}G_{Zn:Ca} = 26650 + 0.66667{}^{\circ}G_{Zn} + 0.33333{}^{\circ}G_{Ca} \quad (11) $$

As seen in Eq. (5), many interaction parameters are needed to describe the Laves phase. More can be added if the interactions in both sublattices are considered simultaneously. Due to the stoichiometry of the Mg_2Ca and $MgZn_2$ compounds, and the nonexistence of the Laves phase in the Ca–Zn system, most interaction parameters in the Laves phase are set to be large positive values.

4. Results and discussion

Based solely on the information from the three binary systems, the calculated ternary liquidus projection was close to the experimental data over nearly the entire composition range (see Fig. 5), with the exception of the area around the ternary compound because it is not present in the single combination of the binary systems.

In the present work, only the model parameters for the liquid phase, the Laves phase, and the ternary compound were needed to reproduce the available experimental data. The evaluation of the model parameters of the Mg–Ca–Zn ternary system was performed with the Parrot module [14] in Thermo-Calc [15]. The interaction parameters of the liquid phase, the Laves phase, and the Gibbs energy of the ternary phase can be found in Appendix B.

The ternary system was first optimized with one ternary phase whose composition was that of Paris, i.e. $Ca_2Mg_5Zn_5$. There was some agreement between the experimental data and the calculated phase diagram over most of the system, but there was significant mismatch around the ternary phase.

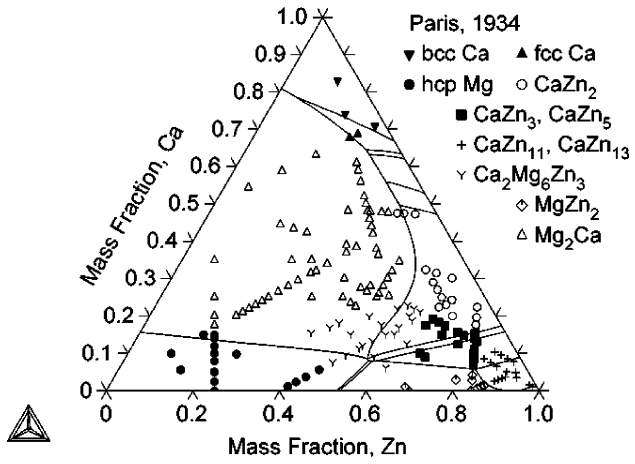

Fig. 5. The calculated Mg–Ca–Zn liquidus projection showing a simple combination of the three binary systems, with Paris' liquidus data for each region superimposed [6].

The ternary system was optimized again with one ternary phase using the composition proposed by Clark and confirmed by Jardim et al. This optimization achieved better results than the previous one using the composition given by Paris. For the sake of comparison, a liquidus projection in Fig. 6 shows the locations of the different proposed ternary phases. The composition of the ternary phase in the calculated liquidus projection in Fig. 6 is $Ca_2Mg_6Zn_3$, proposed by Clark [8] and Jardim et al. [11]. Note that although Clark's beta compound was modeled as a stoichiometric phase in this work, the symbols for the beta compound serve as an approximate boundary for his proposed homogeneity range.

The final calculated Mg–Ca–Zn liquidus projection can be seen in Fig. 7, with the experimental data of Paris superimposed on the diagram [5]. The different symbols denote the different primary phases forming from the liquid phase. A close-up view of the liquidus projection near the middle of the Mg–Zn axis is shown in Fig. 8. The Mg_2Zn_{11} compound is present in the liquidus projection, but it must be plotted on a very small scale to be seen (see Fig. 9). Another liquidus projection is shown in Fig. 10, with the calculated isotherms superimposed on the diagram. The temperatures and liquid compositions of all the invariant reactions on the liquidus were calculated and are listed in Table 1 in order of descending temperature.

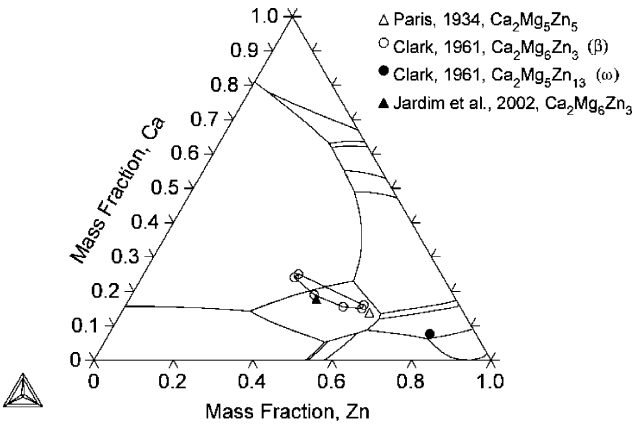

Fig. 6. A Mg–Ca–Zn liquidus projection showing the location of the ternary compounds proposed in the literature [5–9,11].

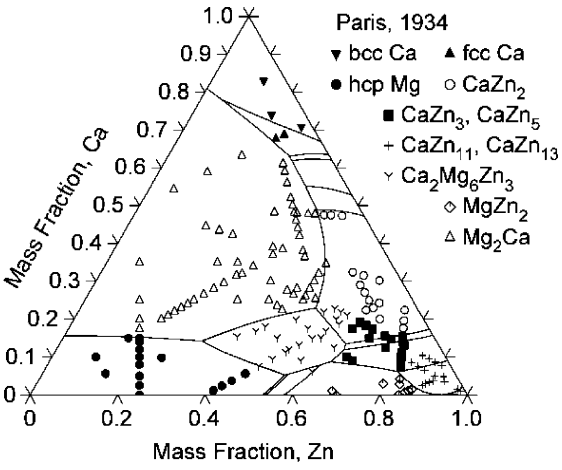

Fig. 7. The calculated liquidus projection, with Paris' liquidus data for each region superimposed [6].

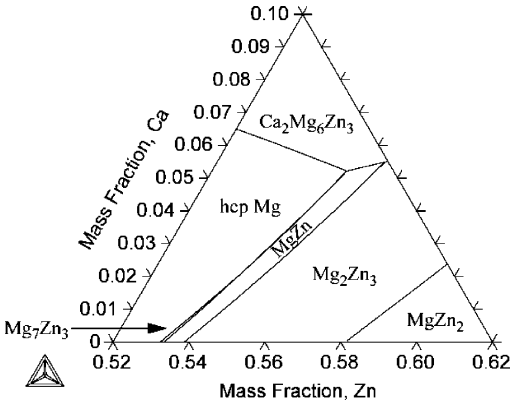

Fig. 8. Close-up of the Mg–Ca–Zn liquidus projection near the middle of the Mg–Zn axis.

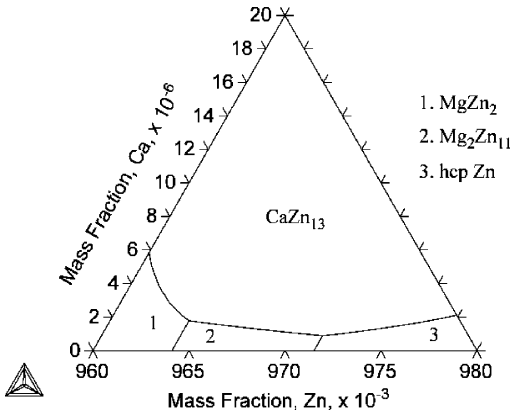

Fig. 9. Close-up of the Mg–Ca–Zn liquidus projection near the Zn-rich end of the Mg–Zn axis.

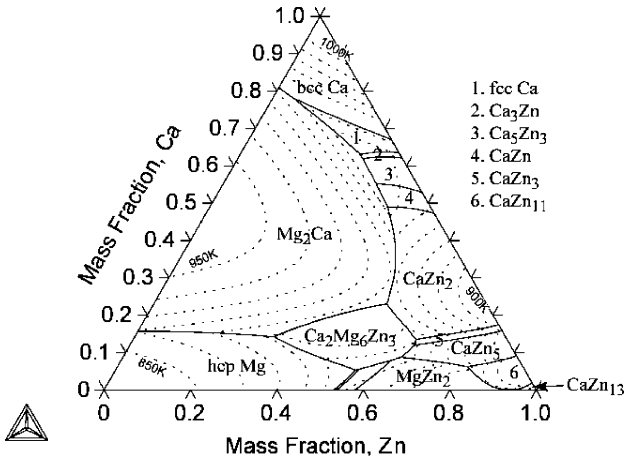

Fig. 10. The calculated liquidus projection, with the calculated isotherms superimposed. The temperature difference between isotherms is 50 K.

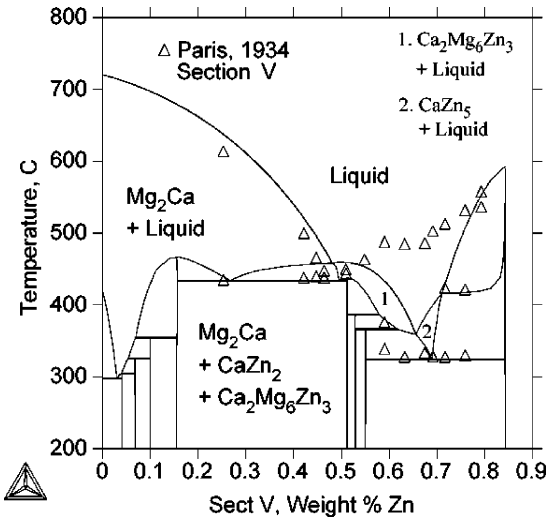

Fig. 11. The calculated isopleth for $w_{Ca} + 0.5931w_{Zn} = 0.5$, compared to the experimental data of Paris. Note the steep drop on the right side of the ternary compound.

Most primary phase regions of solidification measured by Paris were reproduced by the calculations, with the exception of two particular areas. One is the liquidus region in the zinc-rich corner that includes the points marked as "$CaZn_3$,$CaZn_5$", and "$CaZn_{11}$,$CaZn_{13}$". Note that Paris' work does not show the existence of the $CaZn_3$ phase. It was not possible to distinguish which of Paris' data points would correspond to $CaZn_3$ and which ones would correspond to $CaZn_5$, so they were marked by the same symbol in Figs. 5 and 7. Similarly, Paris was unaware of the existence of the $CaZn_{13}$ phase, and the data points corresponding to $CaZn_{11}$ and $CaZn_{13}$ are again marked by the same symbol in Figs. 5 and 7.

The second area that could not be reproduced well is the liquidus of the ternary phase near the Mg–Zn axis. Fig. 11, which is a plot of the Section V isopleth of Paris, clearly illustrates a steep valley running along the Mg–Zn side of the ternary phase. It was impossible to make the ternary phase liquidus agree well with the experimental data. However, it must be noted that the ternary phase was modeled as a stoichiometric compound. If the ternary phase were modeled with some homogeneity range, it is possible that a much better agreement could be obtained. Also note that if the calculated curves were lifted straight up, the region belonging to $CaZn_5$ would not align properly with the liquidus points above it. This serves as circumstantial evidence that a second ternary phase may be present in the system.

During the optimization process, all sixteen of Paris' isopleths were repeatedly plotted to gauge the agreement of the calculated curves with the experimental data. For the sake of brevity, only two of the isopleths are presented here. Fig. 12

Table 1
Invariant liquidus reactions in the Mg–Ca–Zn system

Reaction	Temperature (°C)	Zn (wt.%)	Ca (wt.%)
Liquid + $CaZn_{11}$ → $CaZn_5$ + $MgZn_2$	510.8	81.04	6.15
Liquid + $CaZn_{11}$ → $CaZn_{13}$ + $MgZn_2$	489.9	93.92	2.83×10^{-4}
Liquid + Mg_2Ca + bcc Ca → fcc Ca	442.8	4.31	78.29
Liquid → $CaZn_2$ + Mg_2Ca + $Ca_2Mg_6Zn_3$	433.4	53.91	22.89
Liquid → hcp Mg + Mg_2Ca + $Ca_2Mg_6Zn_3$	415.8	32.26	14.18
Liquid + $CaZn_2$ → $CaZn_3$ + $Ca_2Mg_6Zn_3$	386.1	65.41	13.48
Liquid + $MgZn_2$ + Mg_2Zn_{11} → $CaZn_{13}$	379.7	96.41	1.77×10^{-6}
Liquid + $CaZn_3$ → $CaZn_5$ + $Ca_2Mg_6Zn_3$	366.3	65.88	11.87
Liquid + Mg_2Zn_{11} + Zn → $CaZn_{13}$	364.1	97.15	8.81×10^{-7}
Liquid + $CaZn_2$ → Mg_2Ca + CaZn	354.3	41.09	48.96
Liquid + CaZn → Mg_2Ca + Ca_5Zn_3	325.4	35.47	55.12
Liquid + Mg_7Zn_3 → hcp Mg + MgZn	325.0	54.27	1.96
Liquid + $CaZn_5$ → $MgZn_2$ + $Ca_2Mg_6Zn_3$	323.8	64.36	8.69
Liquid + $MgZn_2$ → Mg_2Zn_3 + $Ca_2Mg_6Zn_3$	318.8	62.52	7.87
Liquid + Ca_5Zn_3 → Mg_2Ca + Ca_3Zn	304.3	29.04	61.81
Liquid → Mg_2Ca + Ca_3Zn + fccCa	303.8	27.77	63.02
Liquid + Mg_2Zn_3 → MgZn + $Ca_2Mg_6Zn_3$	288.1	56.42	5.49
Liquid → hcp Mg + MgZn + $Ca_2Mg_6Zn_3$	282.9	55.56	5.21

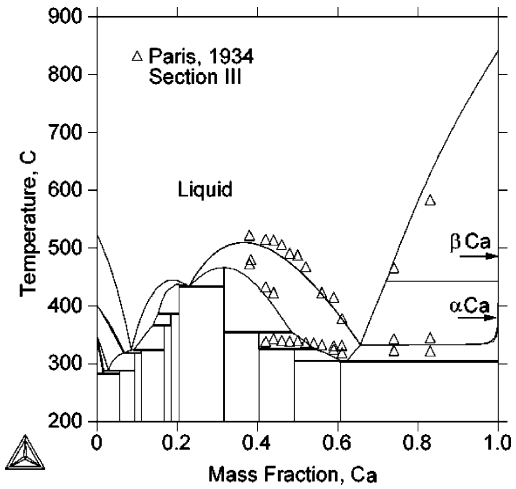

Fig. 12. The calculated isopleth for $w_{Mg} - 0.428w_{Zn} = 0$, compared to the experimental data of Paris [6].

shows Section III, which is defined by the equation

$$w_{Mg} - 0.428w_{Zn} = 0 \quad (12)$$

Fig. 13 shows Section X, which is defined by the equation

$$w_{Ca} - w_{Zn} = 0 \quad (13)$$

Except as noted above, the isopleths presented here, as well as the other fourteen isopleths, show good agreement with the data of Paris.

The present work is based on the assumption that there is only one ternary compound in the Mg–Ca–Zn system. However, in addition to the findings of Clark, the liquidus data of Paris may indicate the presence of a second ternary phase in the zinc-rich corner of the phase diagram. Some or all of the data points corresponding to $CaZn_3$ and $CaZn_5$ in Fig. 7 may be associated with a second ternary phase. It is worth seeing how the calculated phase diagram changes if a second ternary phase is included in the model. A phase with

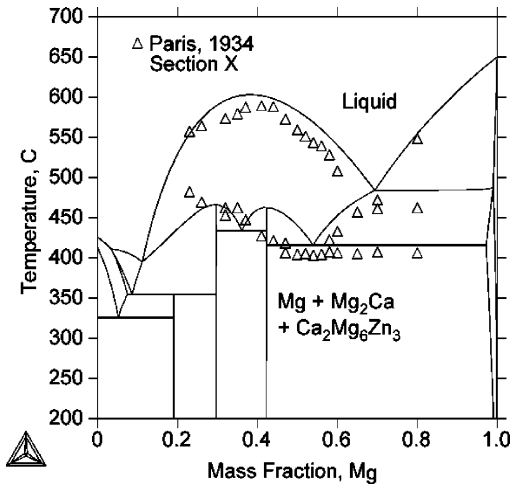

Fig. 13. The calculated isopleth for $w_{Ca} - w_{Zn} = 0$, compared to the experimental data of Paris [6].

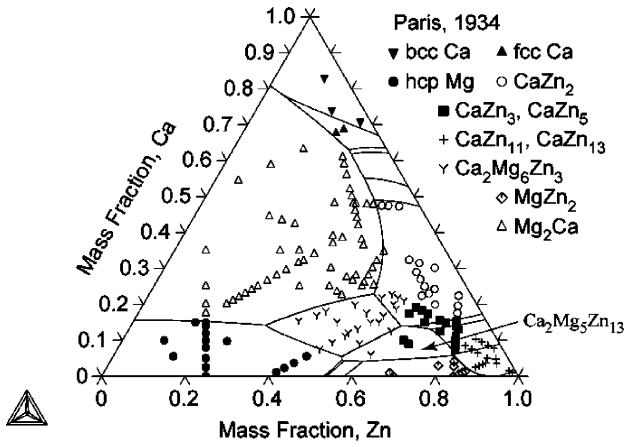

Fig. 14. The calculated liquidus projection, with the presence of two ternary phases, with Paris' liquidus data for each region superimposed [6].

the composition $Ca_2Mg_5Zn_{13}$ was added to the model after the parameters for the liquid and the first ternary phase had been obtained. Because the second ternary phase's composition is near the data points labeled as $CaZn_3$ and $CaZn_5$, the Gibbs energy of the second ternary phase was chosen so as to achieve the best fit with those data points. Fig. 14 shows the resulting liquidus projection, with the Gibbs energy of the second ternary phase being equal to

$$^{\circ}G_m^{Ca_2Mg_5Zn_{13}} = 2^{\circ}G_{Ca}^{bcc} + 5^{\circ}G_{Mg}^{hcp} + 13^{\circ}G_{Zn}^{hcp} - 300000 + 15T \quad (14)$$

As Fig. 14 shows there is partial agreement between the liquidus region of $Ca_2Mg_5Zn_{13}$ and the data points of $CaZn_3$ and $CaZn_5$, yet the remainder of the liquidus projection remains largely unaffected. Fig. 15 shows Section V with two ternary phases present in the calculations. Note that the calculated curve is considerably closer to the experimen-

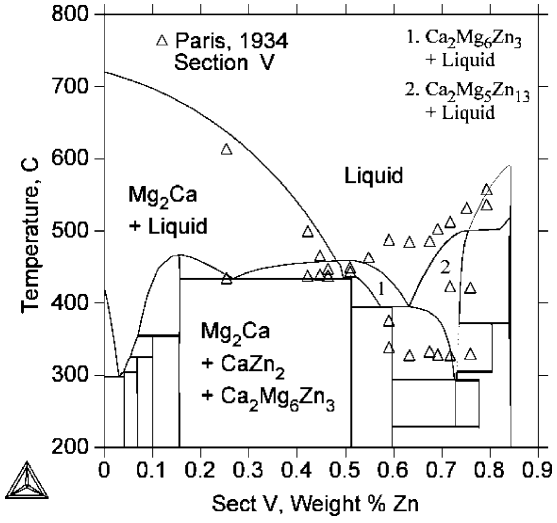

Fig. 15. The calculated isopleth for $w_{Ca} + 0.5931w_{Zn} = 0.5$, with two ternary phases present in the calculation, compared to the experimental data of Paris [6].

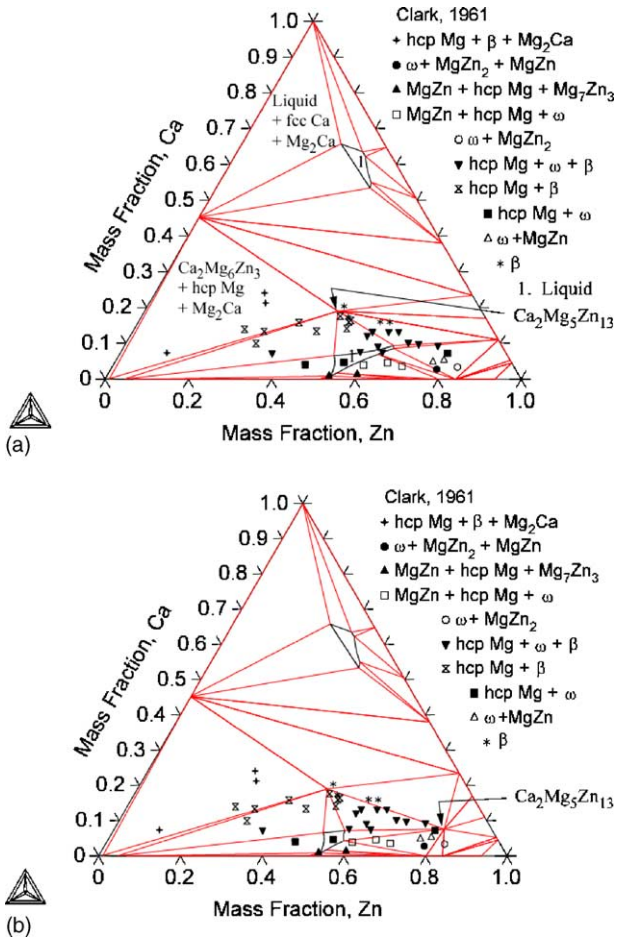

Fig. 16. (a) The calculated 335 °C isotherm with one ternary compound present. (b) The calculated 335 °C isotherm with two ternary compounds present.

tal data than without the second ternary phase, as can be seen in Fig. 11. This indicates the possible presence of a second ternary phase in the Mg–Ca–Zn ternary system. No amount of manipulation made the calculated curve completely agree with the experimental data, and it is not beyond speculation that if a second ternary phase exists, it may also have a homogeneity range of its own. A thorough experimental investigation of the zinc-rich corner of the Mg–Ca–Zn system is needed to verify that a second ternary phase exists in the system, and to accurately determine the phase's composition.

Fig. 16(a) shows the calculated 335 °C isothermal section of the Mg–Ca–Zn system with only one ternary compound in the system. The superimposed data points correspond to the different single- and two-phase regions documented by Clark [7]. There appears to be a minimal correlation between the calculated diagram and Clark's data. Fig. 16(b) shows the same isothermal section with two ternary compounds in the model. There is only a minor improvement in the correlation between Clark's data and the calculated diagram when a second ternary compound is included in the model.

5. Conclusion

Computational thermodynamic modeling of the Mg–Ca–Zn ternary system was performed, and the results of the calculations were compared to the experimental data. One ternary stoichiometric compound was considered for the model, and its Gibbs energy was evaluated. The calculated phase diagram exhibits good agreement with the experimental data. The thermodynamic model of the Mg–Ca–Zn ternary system will contribute to the thermodynamic modeling of multicomponent magnesium alloys. The presence of a second ternary stoichiometric compound was speculated, and its inclusion in the model showed some agreement with the experimental data. However, more experimental data are needed to confirm the existence of a second ternary phase, and to better define its composition.

Acknowledgements

This work was supported by the National Science Foundation under grant DMR-9983532 and a University Fellowship from The Pennsylvania State University. The Thermo-Calc Program is licensed from The Foundation for Computational thermodynamics, Stockholm, Sweden.

Appendix A. Crystallographic data

Crystallographic data of the Mg–Ca system

Phase	Composition (Ca (at.%))	Pearson symbol	Space group	Struktur–Bericht designation	Reference
Mg	0	hP2	$P6_3/mmc$	A3	[16]
βCa	0	cI2	$Im\bar{3}m$	A2	[17]
αCa	0	cF4	$Fm\bar{3}m$	A1	[16]
Mg_2Ca	33.3	hP12	$P6_3/mmc$	C14	[18]

Crystallographic data of the Mg–Zn system

Phase	Composition (Zn (at.%))	Pearson symbol	Space group	Struktur–Bericht designation	Reference
Zn	100	hP2	$P6_3/mmc$	A3	[16]
Mg_7Zn_3	30	oI142	$Immm$	$D7_b$	[16]
MgZn	50	–	–	–	[19]
Mg_2Zn_3	60	mC110	$B2/m$	–	[20]
$MgZn_2$	66–67.1	hP12	$P6_3/mmc$	C14	[21]
Mg_2Zn_{11}	84.6	cP39	$Pm\bar{3}$	$D8_c$	[22]

Crystallographic data of the Ca–Zn system

Phase	Composition (Zn (at.%))	Pearson symbol	Space group	Struktur–Bericht designation	Reference
Ca_3Zn	25	oC16	$Cmcm$	$E1_a$	[23]
Ca_5Zn_3	37.5	tI32	$I4/mcm$	$D8_l$	[24]
CaZn	50	oC8	$Cmcm$	B_f	[23]
$CaZn_2$	66.7	oI12	$Imma$	–	[25]
$CaZn_3$	∼74 to ∼75.2	hP32	$P6_3/mmc$	–	[23]
$CaZn_5$	∼83.3 to ∼83.9	hP6	$P6/mmm$	$D2_d$	[26]
$CaZn_{11}$	91.7	tI48	$I4_1/amd$	–	[27]
$CaZn_{13}$	92.9	cF112	$Fm\bar{3}c$	–	[28]

Crystallographic data of the Mg–Ca–Zn system

Phase	Composition		Pearson symbol	Space group	Struktur–Bericht designation	Reference
	Ca (at.%)	Zn (at.%)				
$Ca_2Mg_6Zn_3$	18.2	27.3	hP22	$P\bar{3}1c$	–	[11]

Appendix B. Thermodynamic parameters of the Mg–Ca–Zn system (in SI units)

Liquid	Sublattice model (Ca,Mg,Zn) ${}^0L_{\mathrm{Ca,Mg,Zn}} = -7029.7;\ {}^1L_{\mathrm{Ca,Mg,Zn}} = -47787;\ {}^2L_{\mathrm{Ca,Mg,Zn}} = -5437.5$
$Ca_2Mg_6Zn_3$	Sublattice model $(Ca)_2(Mg)_6(Zn)_3$ $G^\circ_{m^{Ca_2Mg_6Zn_3}} = 2G^\circ_{Ca^{fcc}} + 6G^\circ_{Mg^{hcp}} + 3G^\circ_{Zn^{hcp}} - 139077 - 0.8081T$
Laves_C14	Sublattice model $(Mg,Ca,Zn)_{0.66667}(Mg,Ca,Zn)_{0.33333}$ $G^\circ_{Ca:Ca} = 12330 + G^\circ_{Ca^{fcc}};\ G^\circ_{Mg:Mg} = 7720 + G^\circ_{Mg^{hcp}}$ $G^\circ_{Zn:Zn} = 5000 + G^\circ_{Zn^{hcp}}$ $G^\circ_{Ca:Mg} = 26650 + 0.66667G^\circ_{Ca^{fcc}} + 0.33333G^\circ_{Mg^{hcp}}$ $G^\circ_{Mg:Ca} = -22624.9 + 155.5042T - 27.57338T\ln T - 0.0015874T^2 + 210000T^{-2}$ $G^\circ_{Ca:Zn} = 26650 + 0.66667G^\circ_{Ca^{fcc}} + 0.33333G^\circ_{Zn^{hcp}}$ $G^\circ_{Zn:Ca} = 26650 + 0.33333G^\circ_{Ca^{fcc}} + 0.66667G^\circ_{Zn^{hcp}}$ $G^\circ_{Mg:Zn} = 29389.65 - 13.644T - 0.66667G_{Mg^{Liq}} - 0.33333G_{Zn^{Liq}} + G^\circ_{Mg^{hcp}} + G^\circ_{Zn^{hcp}}$ $G^\circ_{Zn:Mg} = -19389.65 + 13.644T + 0.33333G_{Mg^{Liq}} + 0.66667G_{Zn^{Liq}}$ All $G^\circ_{i,j:k} = G^\circ_{i:j,k} = 16000$ except: $G^\circ_{Mg,Zn:Mg} = 11666.7;\ G^\circ_{Mg,Zn:Zn} = 11666.7$ $G^\circ_{Mg:Mg,Zn} = 2666.7;\ G^\circ_{Zn:Mg,Zn} = 2666.7$

References

[1] R. Agarwal, J.J. Lee, H.L. Lukas, F. Sommer, Z. Metallkd. 86 (1995) 103.
[2] I. Ansara, A.T. Dinsdale, M.H. Rand (Eds.), COST 507: Thermochemical Database for Light Metal Alloys, vol. 2, European Commission, 1998.
[3] C.O. Brubaker, Z.-K. Liu, CALPHAD 25 (2001) 381.
[4] A.T. Dinsdale, CALPHAD 15 (1991) 317.
[5] R. Paris, Comptes rendus hebdomadaires des saeances de L'Acadamie des Sciences 197 (1933) 1634.
[6] R. Paris, Publications Scientifiques et Techniques du Minist'ere de L'Air, Ministère de L'Air, 1934, pp. 1–86.
[7] J.B. Clark, Trans. AIME 221 (1961) 644.
[8] J.B. Clark, JCPDS Card 12-266, 1961.
[9] J.B. Clark, JCPDS Card 12-569, 1961.
[10] P. Villars, A. Prince, H. Okamoto (Eds.), Handbook of Ternary Alloy Phase Diagrams, vol. 6, ASM International, 1995.
[11] P.M. Jardim, G. Solorzano, J.B.V. Sande, Mircosc. Microanal. 8 (2002) 487.
[12] O. Redlich, A.T. Kister, Ind. Eng. Chem. 40 (1948) 345.
[13] Y. Zhong, Personal communication, 2003.
[14] B. Jansson, Evaluation of Parameters in Thermochemical Models Using Different Types of Experimental Data Simultaneously, TRITA-MAC-0234, Royal Institute of Technology, Stockholm, Sweden, 1984.
[15] B. Sundman, J. Agren, J. Phys. Chem. Solids 42 (1981) 297.
[16] H.W. King, Bull. Alloy Phase Diagrams 2 (1981) 401.
[17] H.W. King, Bull. Alloy Phase Diagrams 3 (1982) 275.
[18] H. Witte, Naturwissenschaften 25 (1937) 795.
[19] K.P. Anderko, E.J. Klimek, D.W. Levinson, W. Tostocker, Trans. ASM 499 (1957) 778.
[20] J.B. Clark, F.N. Rhines, Trans. AIME 209 (1957) 6.
[21] J.B. Friauf, Phys. Rev. 29 (1927) 34.
[22] S. Samson, Acta Chem. Scand. 3 (1949) 835.
[23] M.L. Fornasini, F. Merlo, Acta Crystallogr. B36 (1980) 1739.
[24] G. Bruzzone, E. Franceschi, F. Merlo, J. Less-Common Met. 60 (1978) 59.
[25] G.E.R. Schulze, J. Wieting, Z. Metallkd. 52 (1961) 743.
[26] W. Haucke, Z. Anorg. Chem. 244 (1940) 17.
[27] A. Iandelli, A. Palenzona, J. Less-Common Met. 12 (1967) 333.
[28] J.A.A. Ketelaar, J. Chem. Phys. 5 (1937) 668.